STED properties of Ce3+, Tb3+, and Eu3+ doped inorganic scintillators

M. S. Alekhin, J. Renger, M. Kasperczyk, P. -A. Douissard, T. Martin, Y. Zorenko, D. A. Vasil'Ev, M. Stiefel, L. Novotny, M. Stampanoni

Research Article | Vol. 25, No. 2 | 23 Jan 2017 | OPTICS EXPRESS 1251

Optics EXPRESS

STED properties of Ce^{3+}, Tb^{3+}, and Eu^{3+} doped inorganic scintillators

M. S. ALEKHIN,[1,2,*] J. RENGER,[3] M. KASPERCZYK,[3] P.-A. DOUISSARD,[4] T. MARTIN,[4] Y. ZORENKO,[5] D. A. VASIL'EV,[6] M. STIEFEL,[7] L. NOVOTNY,[3] AND M. STAMPANONI[1,2]

[1]*Institute for Biomedical Engineering, ETH Zürich, Zürich, Switzerland*
[2]*Swiss Light Source, Paul Scherrer Institut, Villigen, Switzerland*
[3]*Photonics Laboratory, ETH Zürich, Zürich, Switzerland*
[4]*European Synchrotron Radiation Facility, Grenoble, France*
[5]*Uniwersytet Kazimierza Wielkiego w Bydgoszczy, Institute of Physics, Bydgoszcz, Poland*
[6]*Prokhorov General Physics Institute, Russian Academy of Sciences, Moscow, Russia*
[7]*EMPA, Dubendorf, Switzerland*
[*]*mikhail.alekhin@alumni.ethz.ch*

Abstract: Scintillator-based X-ray imaging is a powerful technique for noninvasive real-space microscopic structural investigation such as synchrotron-based computed tomography. The resolution of an optical image formed by scintillation emission is fundamentally diffraction limited. To overcome this limit, stimulated scintillation emission depletion (SSED) X-ray imaging, based on stimulated emission depletion (STED) microscopy, has been recently developed. This technique imposes new requirements on the scintillator material: efficient de-excitation by the STED-laser and negligible STED-laser excited luminescence. In this work, luminescence depletion was measured in several commonly-used Ce^{3+}, Tb^{3+}, and Eu^{3+} - doped scintillators using various STED lasers. The depletion of Tb^{3+} and Eu^{3+} via 4f-4f transitions was more efficient (P_s = 8…19 mW) than Ce^{3+} depletion via 5d-4f transitions (P_s = 43…45 mW). Main origins of STED-laser excited luminescence were one- and two-photon excitation, and scintillator impurities. LSO:Tb scintillator and a 628 nm cw STED-laser is the most promising combination for SSED satisfying the above-mentioned requirements.

OCIS codes: (170.6280) Spectroscopy, fluorescence and luminescence; (160.5690) Rare-earth-doped materials; (100.6640) Superresolution; (180.2520) Fluorescence microscopy; (310.6845) Thin film devices and applications; (140.5680) Rare earth and transition metal solid-state lasers.

References and links

1. A. Koch, C. Raven, P. Spanne, and A. Snigirev, "X-ray imaging with submicrometer resolution employing transparent luminescent screens," J. Opt. Soc. Am. A **15**(7), 1940–1951 (1998).
2. M. S. Alekhin, G. Patton, C. Dujardin, P.-A. Douissard, M. Lebugle, L. Novotny, and M. Stampanoni, "Stimulated scintillation emission depletion X-ray imaging," Opt. Express **25**(2), 654 (2017).
3. S. W. Hell and J. Wichmann, "Breaking the diffraction resolution limit by stimulated emission: stimulated-emission-depletion fluorescence microscopy," Opt. Lett. **19**(11), 780–782 (1994).
4. S. W. Hell, "Far-field optical nanoscopy," Science **316**(5828), 1153–1158 (2007).
5. T. Martin and A. Koch, "Recent developments in X-ray imaging with micrometer spatial resolution," J. Synchrotron Radiat. **13**(2), 180–194 (2006).
6. C. Webb and J. Jones, *Handbook of Laser Technology and Applications* (CRC Press, 2003).
7. R. Kolesov, R. Reuter, K. Xia, R. Stöhr, A. Zappe, and J. Wrachtrup, "Super-resolution upconversion microscopy of praseodymium-doped yttrium aluminum garnet nanoparticles," Phys. Rev. B **84**(15), 153413 (2011).
8. R. Wu, Q. Zhan, H. Liu, X. Wen, B. Wang, and S. He, "Optical depletion mechanism of upconverting luminescence and its potential for multi-photon STED-like microscopy," Opt. Express **23**(25), 32401–32412 (2015).
9. C. T. Xu, Q. Zhan, H. Liu, G. Somesfalean, J. Qian, S. He, and S. Andersson-Engels, "Upconverting nanoparticles for pre-clinical diffuse optical imaging, microscopy and sensing: Current trends and future challenges," Laser Photonics Rev. **7**(5), 663–697 (2013).
10. K. I. Willig, B. Harke, R. Medda, and S. W. Hell, "STED microscopy with continuous wave beams," Nat. Methods **4**(11), 915–918 (2007).

#281488 http://dx.doi.org/10.1364/OE.25.001251
Journal © 2017 Received 2 Dec 2016; revised 11 Jan 2017; accepted 12 Jan 2017; published 17 Jan 2017

Optics EXPRESS

11. P. Dorenbos, "Fundamental Limitations in the Performance of Ce3+ -, Pr3+ -, and Eu2+ - Activated Scintillators," IEEE Trans. Nucl. Sci. **57**(3), 1162–1167 (2010).
12. U. Resch-Genger, M. Grabolle, S. Cavaliere-Jaricot, R. Nitschke, and T. Nann, "Quantum dots versus organic dyes as fluorescent labels," Nat. Methods **5**(9), 763–775 (2008).
13. A. N. Butkevich, G. Y. Mitronova, S. C. Sidenstein, J. L. Klocke, D. Kamin, D. N. H. Meineke, E. D'Este, P.-T. Kraemer, J. G. Danzl, V. N. Belov, and S. W. Hell, "Fluorescent rhodamines and fluorogenic carbopyronines for super-resolution STED microscopy in living cells," Angew. Chem. Int. Ed. Engl. **55**(10), 3290–3294 (2016).
14. D. J. Ehrlich, P. F. Moulton, and R. M. Osgood, Jr., "Ultraviolet solid-state Ce:YLF laser at 325 nm," Opt. Lett. **4**(6), 184–186 (1979).
15. P. Rambaldi, R. Moncorgé, J. P. Wolf, C. Pédrini, and J. Y. Gesland, "Efficient and stable pulsed laser operation of Ce:LiLuF4 around 308 nm," Opt. Commun. **146**(1-6), 163–166 (1998).
16. C. D. Marshall, J. A. Speth, S. A. Payne, W. F. Krupke, G. J. Quarles, V. Castillo, and B. H. T. Chai, "Ultraviolet laser emission properties of Ce3+-doped LiSrAlF6 and LiCaAlF6," J. Opt. Soc. Am. B **11**(10), 2054–2065 (1994).
17. L. Kastrup and S. W. Hell, "Absolute optical cross section of individual fluorescent molecules," Angew. Chem. Int. Ed. Engl. **43**(48), 6646–6649 (2004).
18. E. Rittweger, B. R. Rankin, V. Westphal, and S. W. Hell, "Fluorescence depletion mechanisms in super-resolving STED microscopy," Chem. Phys. Lett. **442**(4-6), 483–487 (2007).
19. A. Cecilia, V. Jary, M. Nikl, E. Mihokova, D. Hänschke, E. Hamann, P. A. Douissard, A. Rack, T. Martin, B. Krause, D. Grigorievc, T. Baumbach, and M. Fiederle, "Investigation of the luminescence, crystallographic and spatial resolution properties of LSO:Tb scintillating layers used for X-ray imaging applications," Radiat. Meas. **62**, 28–34 (2014).
20. Z. Marton, H. B. Bhandari, C. Brecher, S. R. Miller, B. Singh, and V. V. Nagarkar, "High efficiency microcolumnar Lu2O3:Eu scintillator thin film for hard X-ray microtomography," JPCS **425**, 062016 (2013).
21. Y. Tatsuya and O. Yasutake, "Amplification and lasing characteristics of Tb 3+ -doped fluoride fiber in the 0.54 μm band," Jpn. J. Appl. Phys. **46**(41), L991–L993 (2007).
22. P. A. Loiko, V. I. Dashkevich, S. N. Bagaev, V. A. Orlovich, A. S. Yasukevich, K. V. Yumashev, N. V. Kuleshov, E. B. Dunina, A. A. Kornienko, S. M. Vatnik, and A. A. Pavlyuk, "Spectroscopic characterization and pulsed laser operation of Eu 3+:KGd(WO 4) 2 crystal," Laser Phys. **23**(10), 105811 (2013).
23. D. K. Sardar, K. L. Nash, R. M. Yow, J. B. Gruber, U. V. Valiev, and E. P. Kokanyan, "Absorption intensities and emission cross sections of Tb3+(4f8) in TbAlO3," J. Appl. Phys. **100**(8), 083108 (2006).
24. Y. Zorenko, V. Gorbenko, I. Konstankevych, B. Grinev, and M. Globus, "Scintillation properties of Lu3Al5O12:Ce single-crystalline films," Nucl. Instrum. Methods Phys. Res. A **486**(1-2), 309–314 (2002).
25. www.crytur.cz
26. D. A. Vasil'ev, D. A. Spassky, V. V. Voronov, V. O. Sokolov, A. V. Khakhalin, N. V. Vasil'eva, and V. G. Plotnichenko, "Effect of Al and Ce ion concentrations on the optical absorption and luminescence in Gd3(Al,Ga)5O12:Ce3+ epitaxial films," Inorg. Mater. **51**(10), 1008–1016 (2015).
27. T. Martin, P. A. Douissard, M. Couchaud, A. Cecilia, T. Baumbach, K. Dupre, and A. Rack, "LSO-based single crystal film scintillator for synchrotron-based hard X-ray micro-imaging," IEEE Trans. Nucl. Sci. **56**(3), 1412–1418 (2009).
28. M. Nikl and A. Yoshikawa, "Recent R&D trends in inorganic single-crystal scintillator materials for radiation detection," Adv. Opt. Mater. **3**(4), 463–481 (2015).
29. I. V. Khodyuk, J. T. M. de Haas, and P. Dorenbos, "Nonproportional response between 0.1-100 keV energy by means of highly monochromatic synchrotron X-Rays," IEEE Trans. Nucl. Sci. **57**(3), 1175–1181 (2010).
30. W. Chewpraditkul, L. Swiderski, M. Moszynski, T. Szczesniak, A. Syntfeld-Kazuch, C. Wanarak, and P. Limsuwan, "Scintillation properties of LuAG:Ce, YAG:Ce and LYSO:Ce crystals for gamma-ray detection," IEEE Trans. Nucl. Sci. **56**(6), 3800–3805 (2009).
31. P.-A. Douissard, A. Cecilia, T. Martin, V. Chevalier, M. Couchaud, T. Baumbach, K. Dupré, M. Kühbacher, and A. Rack, "A novel epitaxially grown LSO-based thin-film scintillator for micro-imaging using hard synchrotron radiation," J. Synchrotron Radiat. **17**(5), 571–583 (2010).
32. Y. Wu, Z. Luo, H. Jiang, F. Meng, M. Koschan, and C. L. Melcher, "Single crystal and optical ceramic multicomponent garnet scintillators: A comparative study," Nucl. Instrum. Methods Phys. Res. A **780**, 45–50 (2015).
33. P. C. Ricci, M. Salis, R. Corpino, C. M. Carbonaro, E. Fortin, and A. Anedda, "A kinetics model for Tb3+ recombinations in low doped Tb:Lu1.8Y0.2SiO5 crystals," J. Appl. Phys. **108**(4), 043512 (2010).
34. S. K. Sharma, S. Som, R. Jain, and A. K. Kunti, "Spectral and CIE parameters of red emitting Gd3Ga5O12:Eu3+ phosphor," J. Lumin. **159**, 317–324 (2015).
35. Y. Zorenko, M. Nikl, V. Gorbenko, V. Savchyn, T. Voznyak, R. Kucerkova, O. Sidletskiy, B. Grynyov, and A. Fedorov, "Growth and luminescent properties of Lu2SiO5 and Lu2SiO5:Ce single crystalline films," Opt. Mater. **33**(6), 846–852 (2011).
36. L. Zheng, G. Zhao, C. Yan, X. Xu, L. Su, Y. Dong, and J. Xu, "Raman spectroscopic investigation of pure and ytterbium-doped rare earth silicate crystals," J. Raman Spectrosc. **38**(11), 1421–1428 (2007).
37. A. A. Kaminskii, H. Rhee, O. Lux, H. J. Eichler, S. N. Bagayev, H. Yagi, K. Ueda, A. Shirakawa, and J. Dong, "Stimulated Raman scattering in "garnet" Lu3Al5O12 ceramics – a novel host-materiel for Ln- and TM-lasant ions," Laser Phys. Lett. **8**(6), 458–464 (2011).

Optics EXPRESS

38. A. Brenier, A. Suchocki, C. Pedrini, G. Boulon, and C. Madej, "Spectroscopy of Mn4+-doped Ca-substituted gadolinium gallium garnet," Phys. Rev. B Condens. Matter **46**(6), 3219–3227 (1992).
39. J. M. Ogiegło, A. Zych, K. V. Ivanovskikh, T. Jüstel, C. R. Ronda, and A. Meijerink, "Luminescence and energy transfer in Lu3Al5O12 scintillators co-doped with Ce3+ and Tb3+," J. Phys. Chem. A **116**(33), 8464–8474 (2012).
40. H. Suzuki, T. A. Tombrello, C. L. Melcher, and J. S. Schweitzer, "Light emission mechanism of Lu2(SiO4)O:Ce," IEEE Trans. Nucl. Sci. **40**(4), 380–383 (1993).
41. P. S. Peijzel, A. Meijerink, R. T. Wegh, M. F. Reid, and G. W. Burdick, "A complete 4fn energy level diagram for all trivalent lanthanide ions," J. Solid State Chem. **178**(2), 448–453 (2005).
42. S. P. Feofilov, A. B. Kulinkin, T. Gacoin, G. Mialon, G. Dantelle, R. S. Meltzer, and C. Dujardin, "Mechanisms for Ce3+ excitation at energies below the zero-phonon line in YAG crystals and nanocrystals," J. Lumin. **132**(11), 3082–3088 (2012).
43. G. Blasse and B. C. Grabmaier, *Luminescent Materials* (Springer–Verlag Berlin, 1994)
44. G. Amaranath, S. Buddhudu, and F. J. Bryant, "Spectroscopic properties of Tb3+-doped fluoride glasses," J. Non-Cryst. Solids **122**(1), 66–73 (1990).
45. J. Hanne, H. J. Falk, F. Görlitz, P. Hoyer, J. Engelhardt, S. J. Sahl, and S. W. Hell, "STED nanoscopy with fluorescent quantum dots," Nat. Commun. **6**, 7127 (2015).
46. I. A. Shcherbakov, A. I. Zagumennyi, and V. A. Mikhailov, "Rare earth ion lasers Nd3+," in *Handbook of Laser Technology and Applications* (Taylor & Francis, 2003), pp. 353–382.

1. Introduction

In conventional X-ray microtomography, an X-ray beam, penetrating and probing a sample, is absorbed by a scintillator screen where it forms an optical image via spontaneous emission of the X-ray excited luminescence centers [1]. This image is projected on a camera with a standard diffraction limited microscope. To overcome this limit, stimulated scintillation emission depletion (SSED) X-ray imaging technique was recently proposed [2]. Its idea was adopted from stimulated emission depletion (STED) microscopy [3,4]. A doughnut-shaped STED-laser beam is applied to the scintillator screen simultaneously with X-ray excitation. The STED-beam instantly de-excites the excited luminescence centers via stimulated emission, confining the excited scintillator region to the very center of the doughnut. The scintillation signal from this region is registered in a raster-scan mode.

Crucial scintillator requirements for high-resolution X-ray imaging are high density, high effective atomic number (Z_{eff}), and high X-ray-to-optical light conversion efficiency [5]. SSED method imposes two additional requirements: efficient de-excitation of the excited luminescence centers by the STED-laser, and sufficiently weak luminescence excited by the STED-laser itself. To our knowledge, no systematic studies on the depletion properties of scintillation materials exist, although some useful information can be obtained from solid-state lasers [6] or up-conversion nano-probes [7,8] of a similar class of compounds. Therefore, the aim of this work is experimental investigation of the depletion properties of several commonly used in X-ray microtomography scintillators, in particular the Ce^{3+}, Tb^{3+}, or Eu^{3+} doped compounds. Furthermore, lanthanide luminescence centers can themselves be potentially used as nano-probes for STED-microscopy, advantaging in narrow multi-color emission bands, non-blinking, and non-photobleacing [7–9].

The resolution in STED-microscopy is determined by the ratio P_{STED}/P_s, where P_{STED} is the STED-laser power applied to a specimen, and P_s - is the STED laser power at which the probability of the excited luminescence center to be de-excited via stimulated emission is 50%. P_s is given by [10]

$$P_s = \frac{Ahc}{\lambda_{STED}\sigma_{STED}\tau_{fl}} \quad (1)$$

where h, c, A, σ_{STED}, and τ_{fl} are the Planck constant, the speed of light, the doughnut area, the stimulated emission cross-section and the fluorescence lifetime of the luminescence centers respectively. Large σ_{STED} and long τ_{fl} are therefore required for the efficient de-excitation. Ce^{3+} emission is caused by 5d-4f electronic transitions with typical τ_{fl} = 15-100 ns [11], an order of magnitude longer than 1-10 ns of STED organic dyes [12,13]. σ_{STED} of Ce^{3+} is

Optics EXPRESS

10^{-18}…10^{-17} cm^2 [14–16], an order of magnitude smaller than 10^{-17}…10^{-16} cm^2 of STED organic dyes [17,18]. Thus, Ce^{3+}-doped scintillators are expected to be depleted at similar STED-laser powers as STED-organic dyes. Tb^{3+} and Eu^{3+} emission is caused by 4f-4f electronic transitions with typical $\tau_{fl} > 1$ ms [19,20], and $\sigma_{STED} \approx 10^{-20}$…$10^{-22}$ cm^2 [21–23], which might relax the STED-power requirement up to two orders of magnitude.

The paper is structured as follows. In section 2, we introduce the investigated scintillators and the setup for the depletion measurements. In section 3, we present luminescence depletion measurements as a function of STED-laser power. From this, we establish the values of P_s, evaluate the intensities of unwanted STED-laser excited luminescence, and discuss its origins.

2. Experiment

Based on high density, high Z_{eff}, and high X-ray-to-optical light conversion efficiency requirements [2], the following scintillators were selected for the depletion measurements. $Lu_3Al_5O_{12}$ doped with 0.07% at. Ce^{3+} (LuAG:Ce) 2.9 μm thick single-crystalline film (SCF) was grown on a 150 μm YAG substrate with liquid-phase epitaxy (LPE) method from PbO-B_2O_3 flux by Zorenko et al [24]. Lu_2SiO_5 doped with Ce^{3+} (LSO:Ce) 100 μm thick single-crystal (SC) was grown by Crytur [25]. $Gd_{2.96}Ce_{0.03}Al_{3.14}Ga_{1.86}O_{12}$ (GGAG:Ce) SCF was grown on a 130 μm GGAG substrate with LPE method by Vasil'ev et al [26]. Lu_2SiO_5 doped with 12% at. Tb^{3+} (LSO:Tb) 1.6 μm thick single-crystalline film (SCF) was grown on a non-luminescent 170 μm thick substrate with LPE method by Martin et al [27]. $Gd_3Ga_5O_{12}$ doped with 2.5% at. Eu^{3+} (GGG:Eu) 2 μm thick single-crystalline film (SCF) was grown on a 170 μm GGG substrate with LPE method by Martin et al [27]. The scintillation properties of these screens are compiled in Table 1, and their emission spectra are shown in Fig. 1.

Table 1. Scintillation properties of the screens used in the luminescence depletion measurements. Columns from left to right: the thickness of the active layer, the light yield expressed in optical photons per absorbed X-ray energy and corrected for the non-linearity of the X-ray response at 10-20 keV [27–32], and the scintillation decay time [28, 33, 34].

Scintillator	Thickness, μm	Light yield, photons/keV	Decay time, ns
LuAG:Ce	2.9	20	60
LSO:Ce	100	18	40
GGAG:Ce	9	30…36	90…170
LSO:Tb	1.6	28	$1.7 \cdot 10^6$
GGG:Eu	2	17	$0.8 \cdot 10^6$

Optics EXPRESS

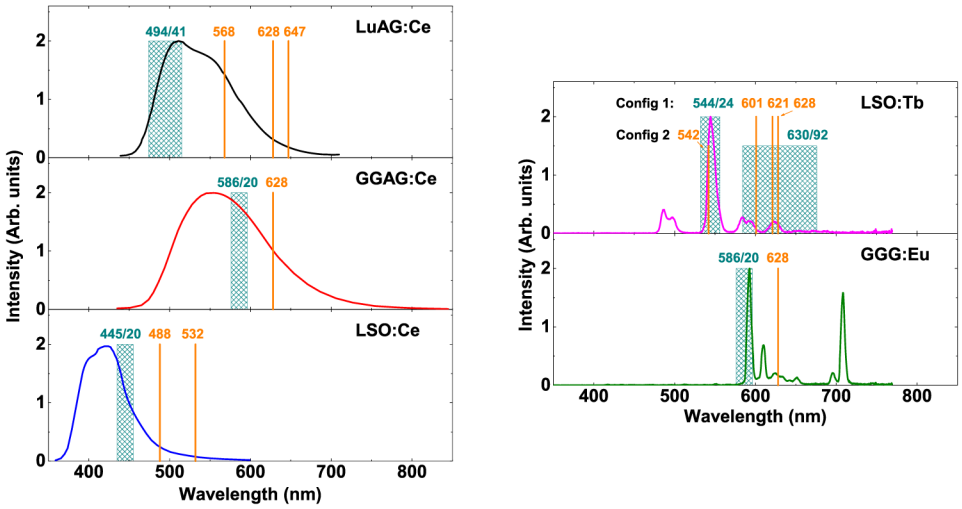

Fig. 1. Emission spectra of LuAG:Ce, GGAG:Ce, LSO:Ce, LSO:Tb, and GGG:Eu scintillators. The spectra were measured with the methods described in the corresponding reports [24, 26, 31, 35]. The vertical lines represent the STED laser wavelengths, and the hatched areas designate the transmission windows of the detection filters used in the depletion measurements.

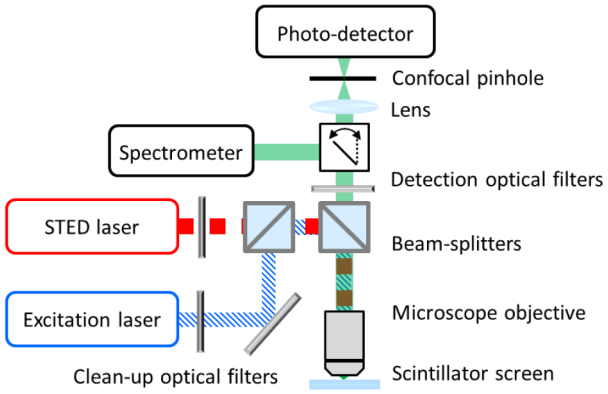

Fig. 2. Schematics of the experimental setup for the luminescence depletion measurements.

The experimental setup for the luminescence depletion measurements is shown in Fig. 2. Excitation and STED Gaussian laser beams were spatially overlapped into the same pathway using a 30:70 and a 90:10 R:T non-polarizing beam-splitters, and focused with a microscope objective (Nikon Plan Apo 40x/0.95NA air) into the same spot on a scintillator screen. Scintillation emission was collected by the same objective and measured by a photo-detector (Micro Photon Devices, SPAD 50 μm, grade C), which also acted as a confocal pinhole. Scattered and reflected excitation and STED photons as well as Raman-scattered STED-laser photons [36–38] were blocked by detection optical filters placed in front of the photodetector. The filters were tilted at 10^0 relative to each other and separated by 2 cm to maximize their optical density (OD) at the excitation and STED laser wavelengths. Emission spectra were measured with a spectrometer (Princeton instruments, Pixis 100B Excelon CCD coupled to a 600 l/mm with 750 nm blaze grating).

Each scintillator was tested with several STED lasers in the following combinations. LuAG:Ce excitation was depleted with 568 nm and 647 nm lines of a Kr-Ar cw-laser (Innova 70C, Coherent inc), and with a 628 nm cw-laser (MPB Communications). GGAG:Ce

Optics EXPRESS

excitation was depleted with the 628 nm laser. LSO:Ce excitation was depleted with a 488 nm line of the Kr-Ar laser and with a 532 nm cw-laser (Verdi V10, Coherent inc). LSO:Tb excitation was depleted with a 542 nm and the 628 nm cw-lasers (MPB Communications), and with 601 and 621 nm lines of a 76.1 MHz fs-pulsed Ti:sapphire pumped OPO laser (Mira-900, Coherent inc). GGG:Eu excitation was depleted with the 628 nm laser. LuAG:Ce, GGAG:Ce, LSO:Ce, and GGG:Eu were excited by a 405 nm cw-laser (CrystaLaser). LSO:Tb was excited by the 488 nm line of the Kr-Ar cw-laser. The scintillator was always positioned with its active layer towards the objective, and the laser was focused through the air inside the scintillator just below the scintillator-air surface. The goal was to have the same spherical aberrations for all the scintillators. This configuration could however enhance the aberrations decreasing actual laser intensity in the confocal volume. The luminescence intensity was measured as a function of STED-laser power multiple times for each combination of scintillator and STED laser. The photo-stability of the scintillators and reproducibility of the results were ensured for several-hour long exposures to < 100 mW STED-lasers.

3. Results and discussion

3.1 Ce^{3+} doped scintillators

The emission of Ce^{3+} in LuAG, GGAG, and LSO consists of two bands due to transitions from the lowest 5d level to the $4f^1$ levels split by 0.27 eV [39–41]. To minimize the excitation by the STED-laser, we adjusted the STED wavelengths to the lower-energy transitions (Fig. 1). The results of LuAG:Ce luminescence depletion measurements are presented in Fig. 3 and Table 2. The depletion was clearly demonstrated with all the STED-lasers. LuAG:Ce luminescence intensity decreased by 20% with 5 mW @ 568 nm, by 65% with 104 mW @ 628 nm, and by 30% with 12.5 mW @ 647 nm. P_s of the 628 nm laser was determined as 45 mW. The depletion curve of the 647 nm STED-laser is not shown in Fig. 3 as it coincides with that of the 628 nm at the studied STED-laser powers.

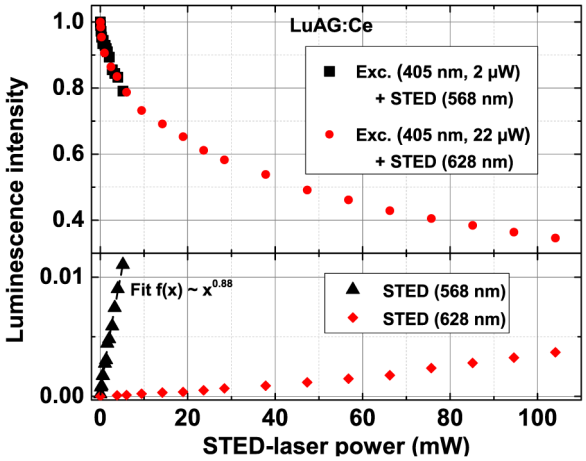

Fig. 3. (Top) LuAG:Ce luminescence intensity excited by the 405 nm laser as a function of 568 nm and 628 nm STED-laser power. (Bottom) LuAG:Ce luminescence intensity excited by the 568 nm and 628 nm STED lasers and normalized to luminescence intensity excited by the 405 nm laser as shown in Appendix A. All laser powers were measured before the objective and corrected for the objective transmittance.

All the lasers excited the scintillator as well. LuAG:Ce emission spectra excited by the 568 nm STED-laser and measured in the 494/41 nm detection window revealed Ce^{3+} emission similar to that in Fig. 1. Its intensity linearly increases with 568 nm laser power, see bottom plot of Fig. 3, which we ascribe therefore to one-photon excitation (OPE). It can be either direct phonon-assisted excitation of Ce^{3+} [42], or excitation of impurities with subsequent

Optics EXPRESS

energy transfer to Ce^{3+} [43]. LuAG:Ce emission spectra excited by the 628 nm and 647 nm lasers revealed only 4f-4f transitions of unwanted Re^{3+} impurities.

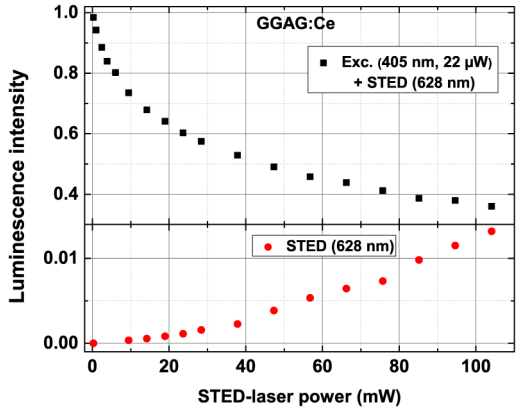

Fig. 4. (Top) GGAG:Ce luminescence intensity excited by the 405 nm laser as a function of 628 nm STED-laser power. (Bottom) GGAG:Ce luminescence intensity excited by the 628 nm STED lasers and normalized to the 405 nm excited luminescence intensity as shown in Appendix A.

GGAG:Ce depletion measurements are shown in Fig. 4. The depletion curve is essentially the same as for LuAG:Ce. The luminescence intensity decreased by 64% with 104 mW @ 628 nm STED-laser, and P_s is 43 mW. GGAG:Ce emission spectra excited by the 628 nm STED-laser and measured in the 494/41 and 586/20 detection windows revealed Ce^{3+} emission similar to that in Fig. 1.

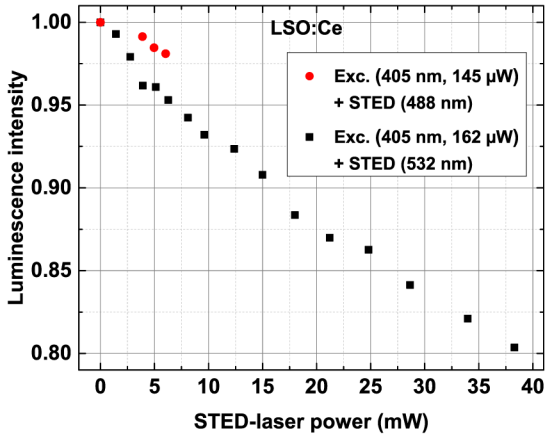

Fig. 5. LSO:Ce luminescence intensity excited by the 405 nm laser as a function of 488 nm and 532 nm STED laser power. The luminescence excited by the STED-laser is negligible.

Figure 5 shows luminescence depletion measurements in LSO:Ce. The luminescence intensity decreased by 2% with 6 mW @ 488 nm of STED-laser, and by 20% - with 38 mW @ 532 nm. The depletion is less efficient compared to LuAG:Ce and GGAG:Ce. We ascribe this to detected out-of-focus luminescence that cannot be depleted [2]. Due to the 100 μm scintillator thickness, its relative fraction in LSO:Ce is the largest among the studied scintillators. The STED-laser excited luminescence signal is 1-3 orders of magnitude lower compared to that of LuAG:Ce and GGAG:Ce. The lowest energy excitation band of LuAG:Ce [39] is separated from the 568, 628, and 647 nm STED-laser lines by 0.57, 0.78, and 0.84 eV respectively. The lowest energy excitation band of LSO:Ce [40] is separated

Optics EXPRESS

from the 532 nm STED-laser line by 0.98 eV. This might explain the observed one-photon excitation in the first case, and its absence in the latter cases.

3.2 Tb^{3+} and Eu^{3+} doped scintillators

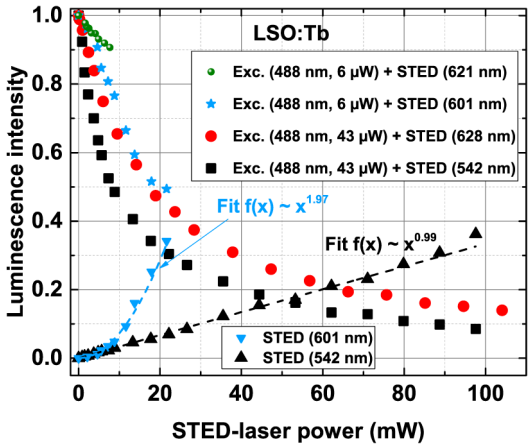

Fig. 6. (Top curves) LSO:Tb luminescence intensity excited by the 488 nm laser as a function of time-averaged power of the 601 nm and 621 nm pulsed STED-lasers and as a function of power of the 542 nm and 628 nm cw STED-lasers. (Bottom curves) LSO:Tb luminescence intensity excited by the 542 nm and 601 nm STED-lasers and normalized to the 488 nm excited luminescence intensity as shown in Appendix A.

The scintillation mechanism of LSO:Tb includes emission from the 4f[$^5D_3$] and 4f[$^5D_4$] levels of Tb^{3+}. Both levels should therefore be de-excited for efficient SSED X-ray imaging. If Tb^{3+} concentration in the crystal is high enough (e.g. > 8% in the melt [19]), spontaneous emission rate from the $^5D_3$ level becomes negligible compared to the $^5D_3$ de-excitation rate via cross-relaxation to the $^5D_4$ level [33]. Almost all the scintillation is then due to $^5D_4 \rightarrow {}^7F_x$ emission transitions, and only $^5D_4$ level of Tb^{3+} must be de-excited with a STED laser for the efficient depletion.

The depletion measurements were performed in two configurations of STED-lasers and emission filters (Fig. 1). In one, we employed the $^5D_4 \rightarrow {}^7F_4$ (601 nm) and $^5D_4 \rightarrow {}^7F_3$ (621 nm, 628 nm) transitions for stimulated emission depletion of Tb^{3+} excitation, and the $^5D_4 \rightarrow {}^7F_5$ transition for luminescence detection. In another, the $^5D_4 \rightarrow {}^7F_5$ (542 nm) transition was used for STED, and lower-energy transitions - for luminescence detection. The results of the luminescence depletion measurements of LSO:Tb are shown in Fig. 6. The depletion was observed with all the STED-lasers. LSO:Tb luminescence intensity decreased by 91% with 97 mW @ 542 nm, by 51% with 22 mW @ 601 nm, by 10% with 8 mW @ 621 nm, and by 86% with 104 mW @ 628 nm. P_s of LSO:Tb is 8 mW, 19 mW, and 17 mW for the 542 nm, 601 nm, and 628 nm STED-lasers respectively. P_s for 542 nm is twice smaller than P_s for 601 nm and 628 nm apparently due to larger σ_{STED} for the $^5D_4 \rightarrow {}^7F_5$ transition compared to the $^5D_4 \rightarrow {}^7F_{3,4}$ transitions [44].

542 nm and 601 nm STED-lasers cause strong Tb^{3+} luminescence signal due to one- and two-photon excitation (TPE), confirmed by linear and quadratic dependences of the emission intensity on the STED-laser power (Fig. 6). TPE can be avoided by using a cw-laser instead of a fs-pulsed. The 628 nm STED-laser produced one of the weakest luminescence signals among all the studied combinations.

Optics EXPRESS

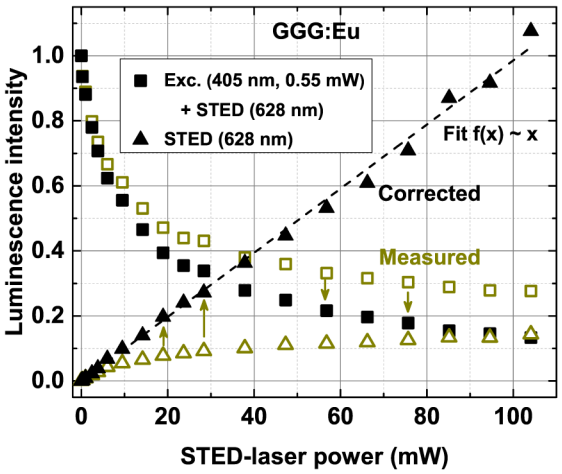

Fig. 7. (Top curves) GGG:Eu luminescence intensity excited by the 405 nm laser as a function of 628 nm STED-laser power. (Bottom curves) GGG:Eu luminescence intensity excited by the 628 nm STED lasers and normalized to the 405 nm excited luminescence intensity. Hollow points are measured values, and solid points are the values corrected for the STED-laser excited luminescence, see Appendix A.

The results of GGG:Eu luminescence depletion measurements are shown in Fig. 7. Its luminescence intensity decreased by 89% with 104 mW @ 628 nm STED-laser. Its P_s = 11 mW is similar to those of LSO:Tb. The STED-laser excited Eu^{3+} luminescence signal is caused by OPE as confirmed by a linear fit of the luminesce intensity. In GGG:Eu, the ratio of the luminescence signal caused by the STED-laser to that caused by the excitation laser is the highest among the studied scintillators. Figure 7 then shows both measured and corrected data to visualize the effect of the STED-laser excited luminescence discussed in Appendix A.

Table 2. Summary of the luminescence depletion measurements. Columns from left to right: the scintillator compound; the STED-laser type and wavelength; STED-laser power at which the luminescence intensity is reduced by half; maximum STED-laser power applied to the scintillator; fraction of luminescence intensity remained at this STED-laser power; measured luminescence signal, excited by the STED laser of this power; main origins of the STED-laser excited luminescence.

Scintillator	STED laser type and λ, nm	P_s, mW	P_{STED}, mW	Luminescence intensity, %	STED-laser excited luminescence	
					Signal, cps	Main origins
LuAG:Ce	568-cw	45	5.2	79	350	OPE + Ce^{3+} emission
	628-cw		104	35	1200	Re^{3+} impurities emission
	647-cw		12.4	70	400	Re^{3+} impurities emission
GGAG:Ce	628-cw	43	104	36	1300	Ce^{3+} emission
LSO:Ce	488-cw		6	98	50	
	532-cw		38	80	2	
LSO:Tb	542-cw	8	97.6	9	1700	OPE + Tb^{3+} emission
	601-pulsed	19	21.6	49	5000	TPE + Tb^{3+} emission
	621-pulsed		7.7	90	15	
	628-cw	17	104	14	10	
GGG:Eu	628-cw	11	104	13	3500	OPE + Eu^{3+} emission

The depletion of the luminescence has been demonstrated in all the studied scintillators. Due to larger product $\sigma_{STED}\tau_{fl}$, the depletion of Tb^{3+} and Eu^{3+} require smaller STED-laser powers (P_s ≈10…20 mW) compared to Ce^{3+} (P_s ≈45 mW). Both are similar to P_s ≈10 mW of STED-nanoscopy fluorescent dyes [10] and P_s ≈50 mW of quantum dots [45]. Due to spherical aberrations, the STED-laser intensity in the confocal volume can be several-fold

Optics EXPRESS

lower than the actual one. In any case, about 50-150 mW of STED-laser power focused into a single doughnut would be required for decent SSED X-ray imaging resolution [2]. To relax the power requirement, one can consider to use e. g. Nd^{3+} transitions [46], or depletion via up-conversion [8].

In synchrotron-based SSED X-ray imaging, the estimated photodetector signal due the scintillation from the doughnut-center is 250 counts per second (cps) for LSO:Ce and 800 cps for LSO:Tb [2]. For the setup used in this work, it would be ~10…80 cps, considering ~10% transmission of the beam-splitter and not optimal detection filters. Table 2 shows that the 628 nm @ 100 mW STED-laser causes 10 cps luminescence signal in LSO:Tb, allowing reasonable signal-to-noise ratio in prospective SSED X-ray imaging. Another promising combination of LSO:Ce with the 532 nm STED-laser require further tests with higher STED-laser power and a thinner sample. Higher purity LuAG:Ce scintillator with 628nm/647nm lasers might also be acceptable for SSED X-ray imaging.

4. Summary

The stimulated emission depletion of luminescence in LuAG:Ce, GGAG:Ce, LSO:Ce, LSO:Tb, and GGG:Eu scintillators was experimentally investigated. The goal was to find a combination of the scintillator and the STED laser with efficient depletion of the excited luminescence centers by the STED-laser and with minimal luminescence excited by the STED-laser itself. Such combinations can be then used in SSED X-ray imaging or in STED-microscopy.

The excitation and the STED-lasers were focused at the same spot on the scintillator screen, and the luminescence intensity was measured as a function of STED-laser power. All the scintillators demonstrated photo-stability over several-hour exposure to < 100 mW STED beams. The depletion was observed in all the scintillators. Tb^{3+} and Eu^{3+} were de-excited more efficiently (P_s = 8…19 mW) compared to Ce^{3+} (P_s = 43…45 mW). This agrees with the smaller product $\sigma_{STED}\tau_{fl}$ of Ce^{3+} 5d-4f transitions, compared to that of Tb^{3+}/Eu^{3+}4f-4f transitions. Since P_s are comparable to those of STED-organic dyes, the studied materials can be potentially applied as nano-probes in STED-microscopy.

The luminescence excited by the STED lasers had several origins. The strongest signals were caused by one- and two-photon excitations of LSO:Tb and GGG:Eu. TPE can be reduced by using e. g. cw STED-lasers instead of fs-pulsed. The intensity of one-photon-excited Ce^{3+} emission in LuAG and LSO become negligible if energy-difference between the lowest 4f-5d excitation band of Ce^{3+} and the STED-photon is at least ≈0.8 eV. Unwanted Re^{3+} impurities, even if not detectable with standard optical excitation, can cause significant STED-laser excited luminescence.

Considering good depletion efficiency and weak STED-laser excited luminescence, LSO:Tb and the 628 nm STED-laser is the best combination for SSED X-ray imaging. Other promising combinations, LSO:Ce + 532 nm laser and LuAG:Ce + 628 nm/647 nm lasers, require further depletion studies.

Appendix A. Correction for the STED-laser excitation

To obtain the luminescence depletion functions of Figs. 3-7, we measured the intensity of the luminescence, excited by the excitation and STED lasers focused on the same spot of the scintillator screen in three different configurations. I_{exc} is the luminescence intensity measured with the excitation laser focused on the screen, and the STED laser blocked. This emission originates from the luminescence centers excited solely by the excitation laser. I_{STED} is the luminescence intensity measured with the STED laser focused on the screen, and the excitation laser blocked. This emission originates from the luminescence centers excited by the STED laser and partially de-excited by the same laser. $I_{exc+STED}$ is the luminescence intensity measured with both the excitation and the STED lasers focused on the screen. This

Optics EXPRESS

emission originates from the luminescence centers excited by both the excitation and the STED lasers, and partially de-excited by the STED laser.

The values of $I_{exc+STED}/I_{exc}$ and I_{STED}/I_{exc} are plotted as hollow squares and hollow triangles in Fig. 7, respectively. $I_{exc+STED} - I_{STED}$ is the intensity of the emission originating from luminescence centers excited by the excitation laser, and partially de-excited by the STED laser. $D = (I_{exc+STED} - I_{STED})/I_{exc}$ then represents the actual depletion effect on the scintillator excitation. Actual luminescence intensity excited by the STED laser is then $I'_{STED} = I_{STED}/D = I_{exc}I_{STED}/(I_{exc+STED} - I_{STED})$. Normalized to I_{exc}, these values $I_{STED}/(I_{exc+STED} - I_{STED})$ are plotted as solid triangles in Figs. 3, 6, and 7. These correction were implemented only in the cases of LuAG:Ce + 568 nm, LSO:Tb + 542 nm, LSO:Tb + 601 nm, and GGG:Eu + 628 nm, where both the excitation and the STED lasers excited the same type of luminescence centers into the same states. In all cases, the measured luminescence intensities were several orders of magnitude below the saturation level.

Funding

ERC grant ERC-2012-StG 310005-PhaseX.

Acknowledgments

LuAG:Ce single crystalline films were grown in a frame of Polish NCN 2016/21/B/ST8/03200 project. The growth of GGAG:Ce was supported by European Social Fund's Doctoral Studies and Internationalisation Programme DoRa. We thank Natalia Vasil'eva and Stefan Stutz for scintillator preparation, Pablo Villanueva for critical comments and Zachary Lapin for help with lasers.